

CHAPTER V

MORE EXPERIMENTAL RESULTS

5.1 Spectra of Fe<sup>57</sup>

The most used isotope in Mössbauer studies is iron-57. This isotope is a decay product of Co<sup>57</sup> which has a half life of 270 days. Co-57 decays into an excited state of Fe<sup>57</sup> via electron capture. Efficiency of this decay route is 99.98%. The decay scheme is shown in Figure 5.1.

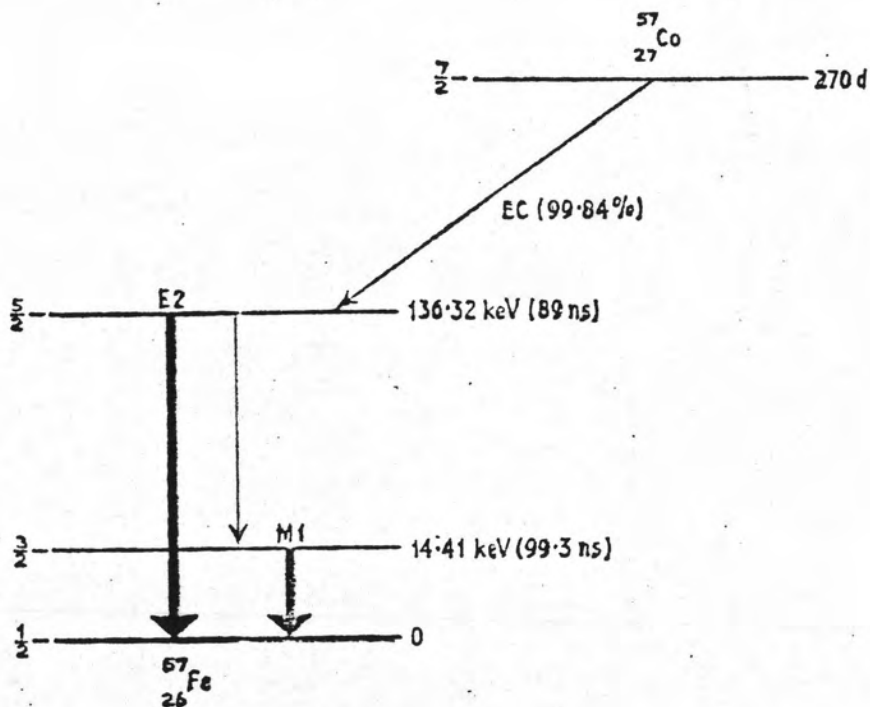


Figure 5.1 The  $\gamma$ -ray scheme of Co<sup>57</sup> showing the 14.41 keV and 136.32 keV transition.

In this Figure, we see that the Co-57 decaying into the  $I=5/2$  state of the Fe-57 nuclei. This state lies at an energy of 136.32 keV above the  $I=1/2$  ground state. The life of this state is 89 nanoseconds. It decays either to the ground state directly or to the  $I=3/2$  state via a 136.32 keV gamma ray (E2 wave) or a 121.91 keV gamma ray. The branching ratio is about 8 for the two decay paths (85% of the time it decays via  $5/2 \rightarrow 3/2$  transition and 11% via the  $5/2 \rightarrow 1/2$  transition). This  $I=3/2$  state lies 14.41 keV above the ground state. The half life of this state is 99.3 nanoseconds and it decays to the ground state via a M1 (14.41 keV ray) transition. The  $3/2 \rightarrow 1/2$  Fe-57 transition when the Fe-57 is in a metallic matrix such as Co, Cr, Pt is a recoilless one and the Lorentzian distribution for the emitted 14.41 keV gamma ray is very narrow one.

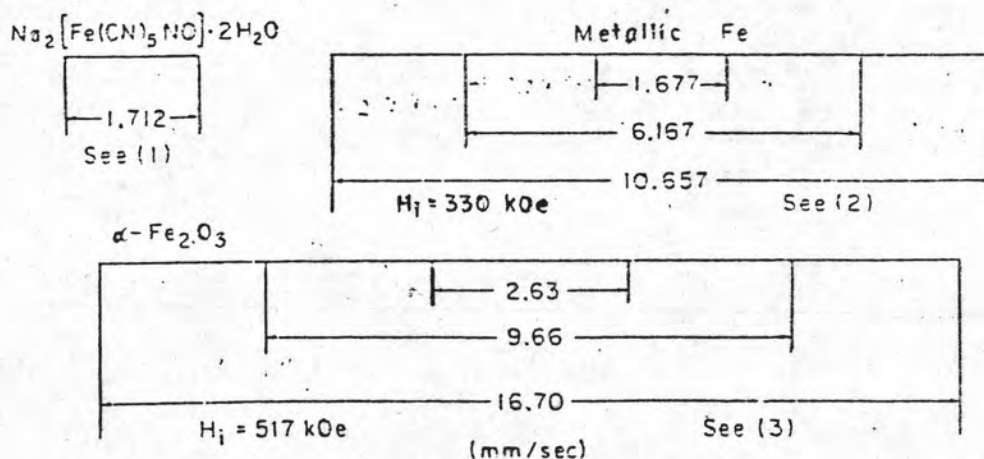


Figure 5.2 Isomer shift (mm/sec) relative to metallic iron.

The center of the distribution is however shifted due to the chemical isomer effect. In Figure 5.2, we see the isomer shifts for various matrices, measured relative to natural iron. In Figure 5.3, we see the magnetic splitting of the nuclear levels of  $\text{Fe}^{57}$ . As we see, the Zeeman splittings of the  $I=3/2$  level produces four states corresponding to  $m = 3/2, 1/2, -1/2$  and  $-3/2$ , while the splitting of the  $I=1/2$  level produces two states corresponding to  $m = -1/2$  and  $+1/2$ . The six transitions indicated in Figure 5.3 correspond to those transitions which would result in changes in  $m$  of  $0, \pm 1$ .

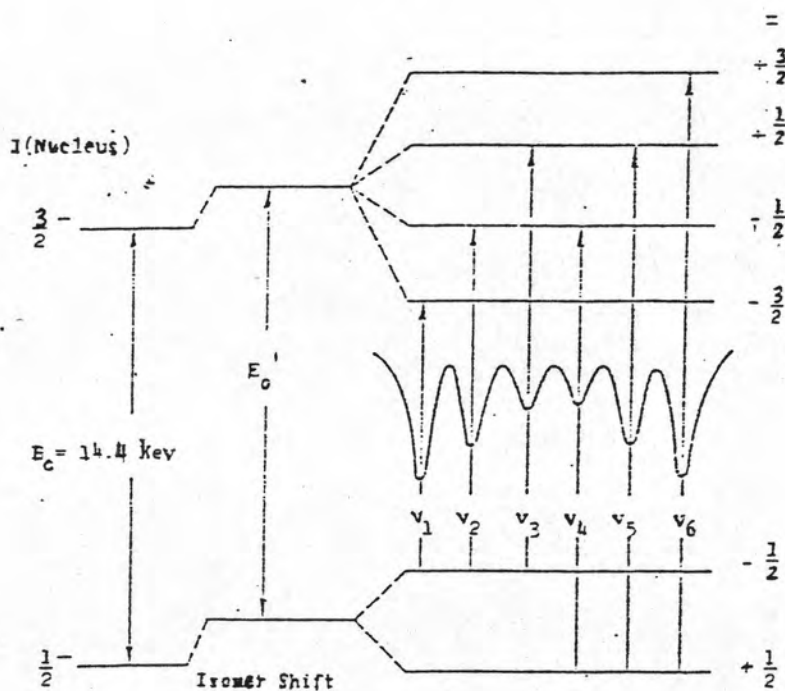


Figure 5.3 Magnetic splitting of nuclear levels in  $\text{Fe}^{57}$ .

The energy of the gamma ray emitted by a  $Fe^{57}$  nuclei embedded in a metallic matrix would be 14.41 keV minus the difference in the isomer shifts of the  $I=3/2$  and  $I=1/2$  levels (Figure 5.2). Since most of the metallic matrices have cubic crystal structures, there is no quadrupole splitting of the  $I=3/2$  level (see Figure 4.5) and only gamma rays of one energy are emitted. Assuming that the energy levels of the  $Fe^{57}$  nuclei in the absorber are split in the way shown in Figure 5.3, absorption of the gamma rays emitted by the source nuclei would only be possible if the Doppler shifted gamma rays of energy

$$E = E_0 (1 + v/c) \quad (5.1)$$

where

$$E_0 = 14.41 \text{ keV} - \text{Isomer shift energy}$$

and  $v$  is the velocity of the source, is equal to energy differences between the levels shown.

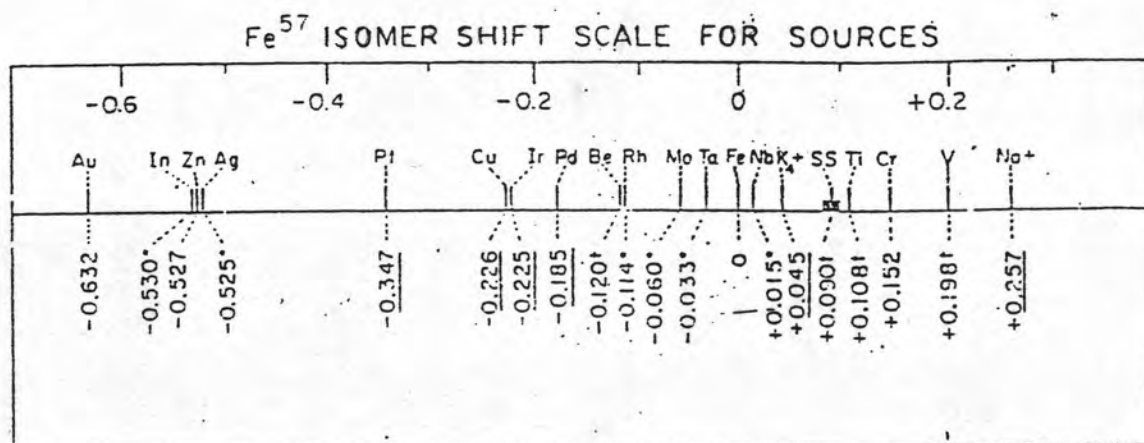


Figure 5.4 Reference splitting useful for calibration.

In Figure 5.4, we see the positions of the six absorption lines for  $\text{Fe}^{57}$  embedded in various systems. By comparing the splitting of six lines for the  $\text{Fe}^{57}$  nuclei in any of the host above for a particular setting of controls in any individual Mössbauer spectrometers, calibration of the spectrometer is instantly achieved

### 5.2 $\text{Fe}^{57}$ Mössbauer Spectra for Yttrium Iron Garnets.

Mössbauer spectroscopy of yttrium iron garnets confirmed that iron goes into the octahedral (a) sites and the tetrahedral (d) sites of the garnets. Because there are two sets of octahedral sites in the garnet structure, three sextets are usually recorded in a Mössbauer study of the YIG's. In Figure 5.5, we show the spectra obtained at 4.2 K and 300 K. In Table 5.1, we see the differences in the parameters of YIG specimens. (15)

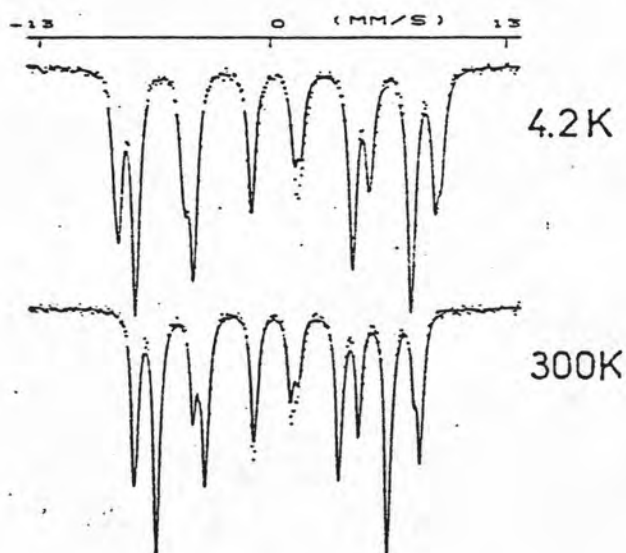


Figure 5.5 Mössbauer spectra recorded at 4.2 K and 300 K on a polycrystalline yttrium iron garnets  $\text{Y}_3\text{Fe}_5\text{O}_{12}$ .

Table 5.1

Information obtained from analysis of the spectra for YIG's.

Lattice site	Temperature (K)	I.S. (mm/s)	$\Gamma$ (mm/s)	$2\epsilon$ (mm/s)	$H_{\text{hyp}}$ kOe
Octahedral sites	4.2	0.44	0.52	-0.01	543
4( $a_2$ )	300	0.33	0.48	-0.03	480
Octahedral sites	4.2	0.47	0.50	0.13	561
12( $a_1$ )	300	0.39	0.34	0.08	497
Tetrahedral sites	4.2	0.25	0.52	0.00	475
24(d)	300	0.16	0.42	0.01	398

The isomer shift I.S. is relative to metallic iron at 300 K.

$\Gamma$  is the linewidth at half-height.

$2\epsilon$  is the quadrupole shift.

### 5.3 Description of Mössbauer Spectrometer Used in This Study.

The Mössbauer spectrometer used in this study belongs to the Department of Physics, Faculty of Science, Mahidol University and is located in the "High Technology" Ceramic Laboratory of Professor Dr. I-Ming Tang. The system consists of

1.  $\text{Co}^{57}$  embedded in palladium as the gamma ray source.
2. A Kr Proportional Counter ( Figure 5.6 ).
3. Mössbauer drive system 'Model 251' from CMTE (Germany) consisting of a velocity transducer drive 'Model 250' and driving unit 'Model 351' (Figure 5.7 and Figure 5.8)
4. A Canberra 'Model 8100' Multichannel Analyzer (MCA) used to set the windows on the timing single channel analyzer TSCA. (Figure 5.9)
5. Multichannel scaling Unit (MCS)/ Multichannel Data Processor 'Model MCD 301/8k' (Figure 5.10)
6. Timing Single Channel Analyzer (TSCA).
7. Monitor and Printer.

The arrangement of the components is shown in Figure 5.11.

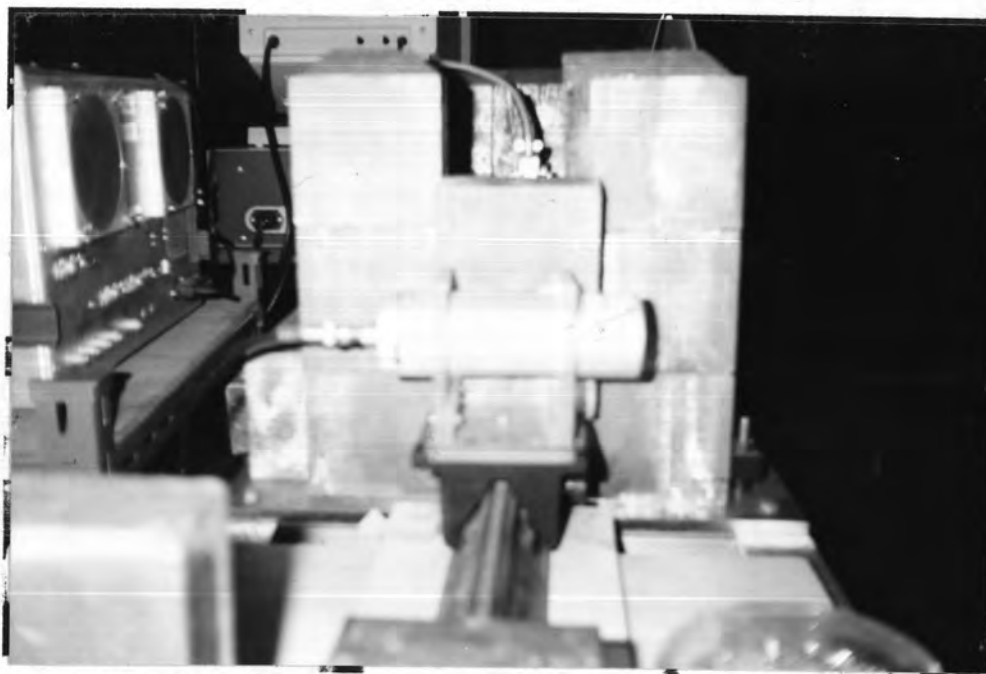


Figure 5.6 Detector.





Figure 5.7 Mössbauer Drive system 'Model 351'.

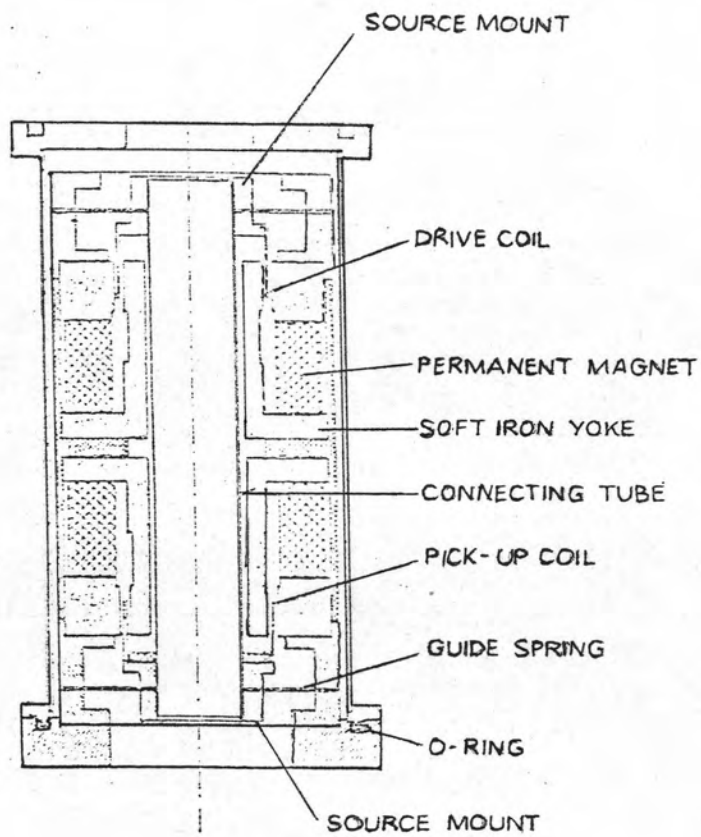


Figure 5.8 Mössbauer Velocity Transducer MA 250.



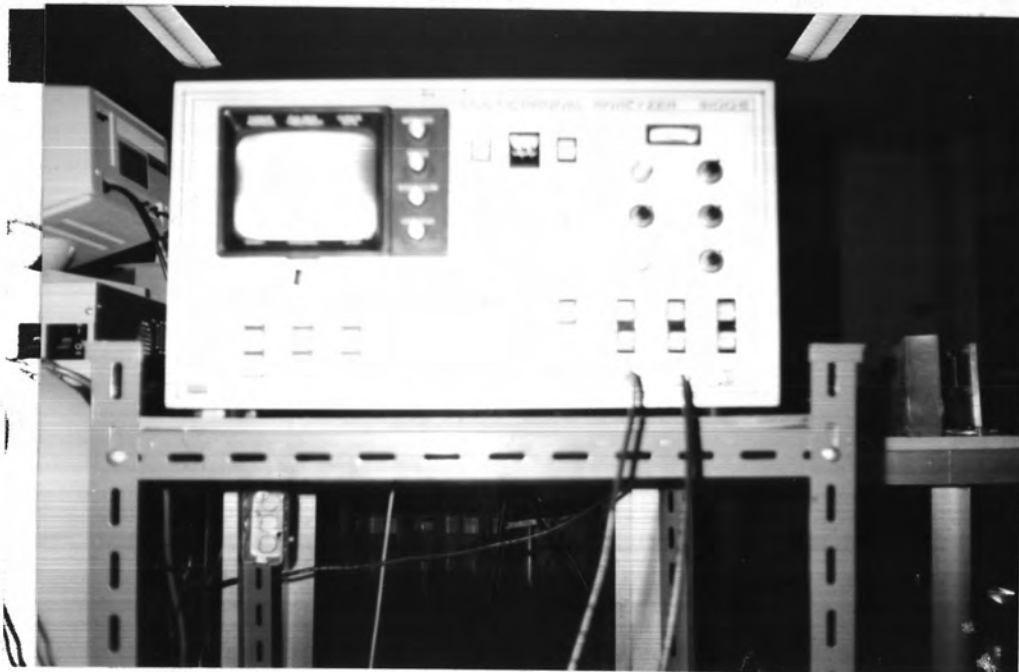


Figure 5.9 Multichannel Analyzer.

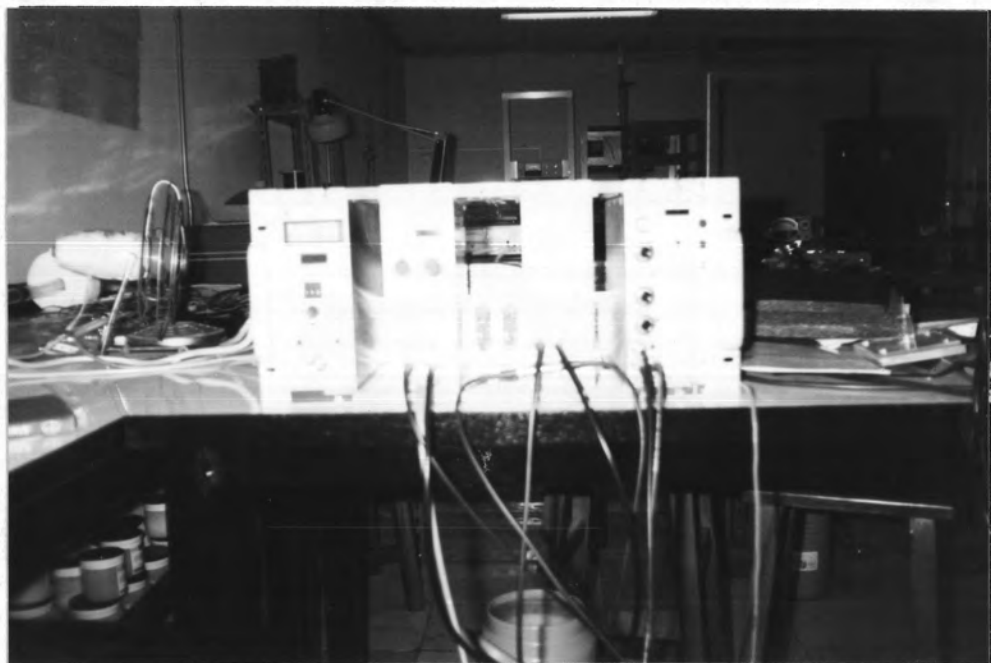


Figure 5.10 TSCA and Multichannel Data Processor.

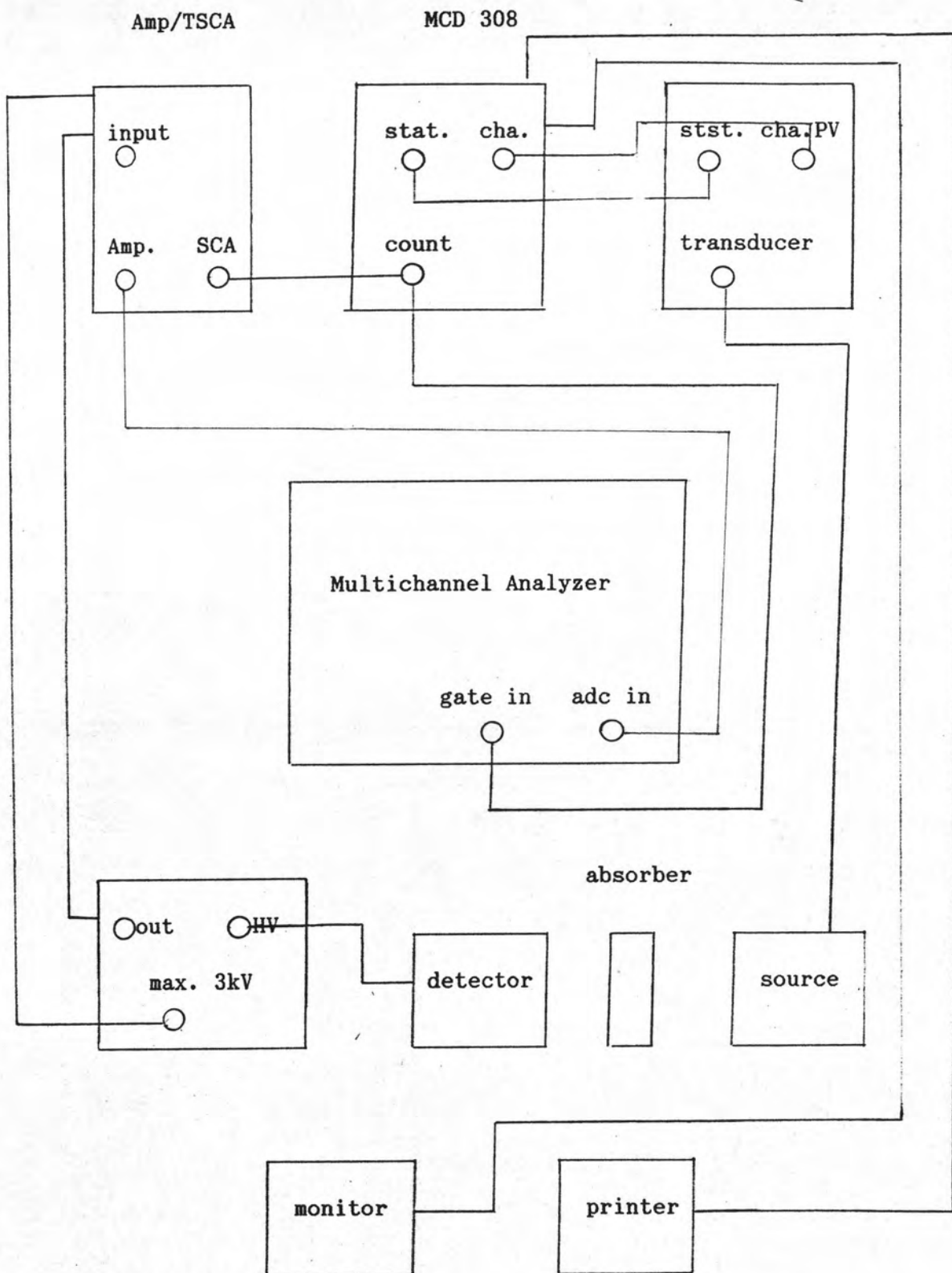


Figure 5.11 Block Diagram of Mössbauer Spectrometer.

#### 5.4 Experimental Procedure

A. The various components were connected together as shown in Figure 5.11

B. The settings on the amplifier (TSCA) and the MCA were set so that only the 14.41 keV gamma ray were recorded. An standard X-ray source was used to accomplish this.

C. The Mössbauer spectra for a natural iron foil was obtained over a twenty four hour period. The Mössbauer spectra for  $\text{Fe}^{57}$  is shown in Figure 5.12.

D. One of the yttrium iron garnet pellets fabricated was ground into fine powder. The powder was then pressed onto a stricky tape covering a copper ring of 2.5 cm diameter. The thickness of the absorber made from the YIG was about 0.05 cm. This was then placed into the spectrometer.

E. The spectrometer collected data for three days. The Mössbauer spectra for the YIG absorber is shown in Figure 5.13.

F. The data was transfered to a computer for data analysis on a IBM compatable PC.

#### 5.5 Results.

The data for the iron foil is listed in Appendix A. The spectra, Figure 5.12, was compared to the reference spectra, Figure 5.4, to establish that with the settings used, each channel recorded the information corresponding to a Doppler shift of

$$\text{velocity/channel} = 0.03 \text{ mm/s}$$

or to a magnetic field width of

1.119 kOe/channel

Based on the splitting between the first and sixth lines in each of the sextets appearing on Figure 5.13 and the determination of the central channel of these lines, we obtain the following results:

Table 5.2  
Isomer Shift and Internal Magnetic Field  
of the Yttrium Iron Garnets Studied.

Lattice Site	Position 1st Peak	Position 6th Peak	Isomer Shift (mm/s)	Hyperfine Field (kOe)
4a	44	470	0.14	477
12a	29	470	0.36	493
24d	80	435	0.12	397

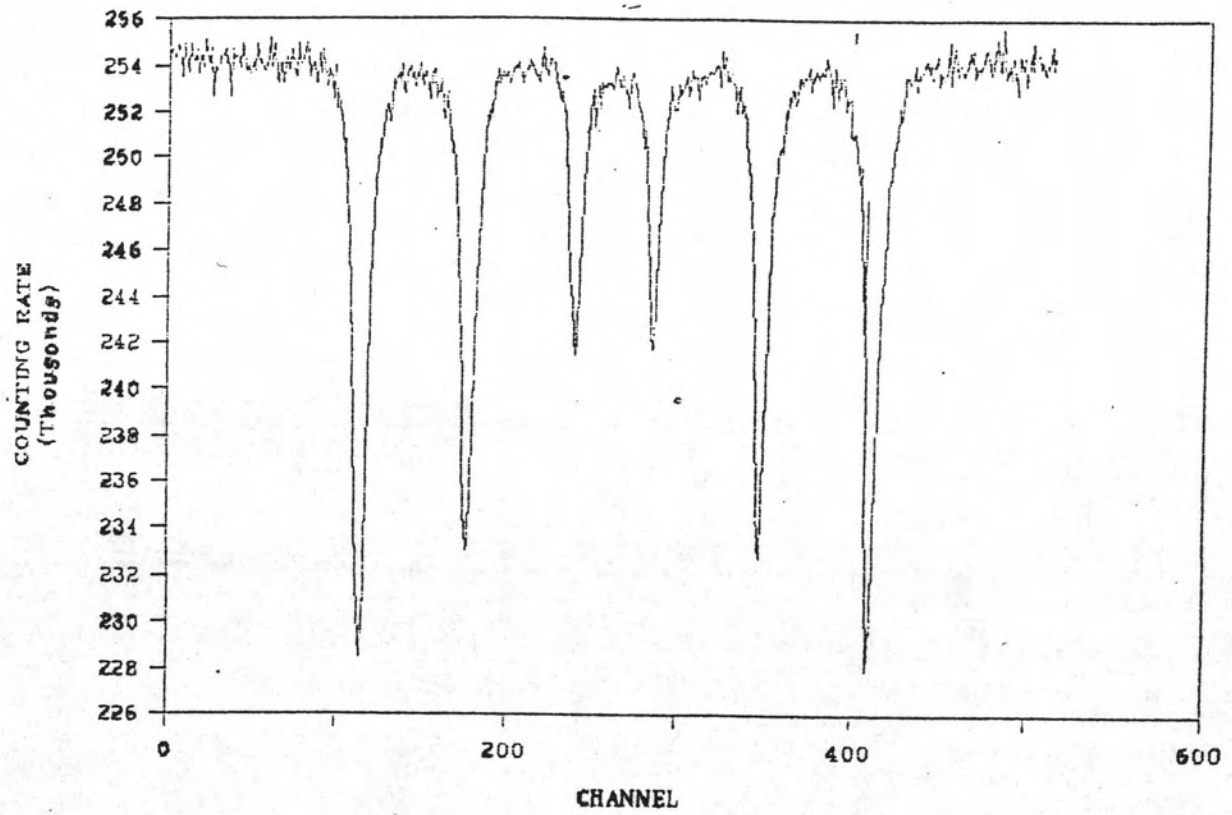


Figure 5.12 The Mössbauer spectra for iron foil.

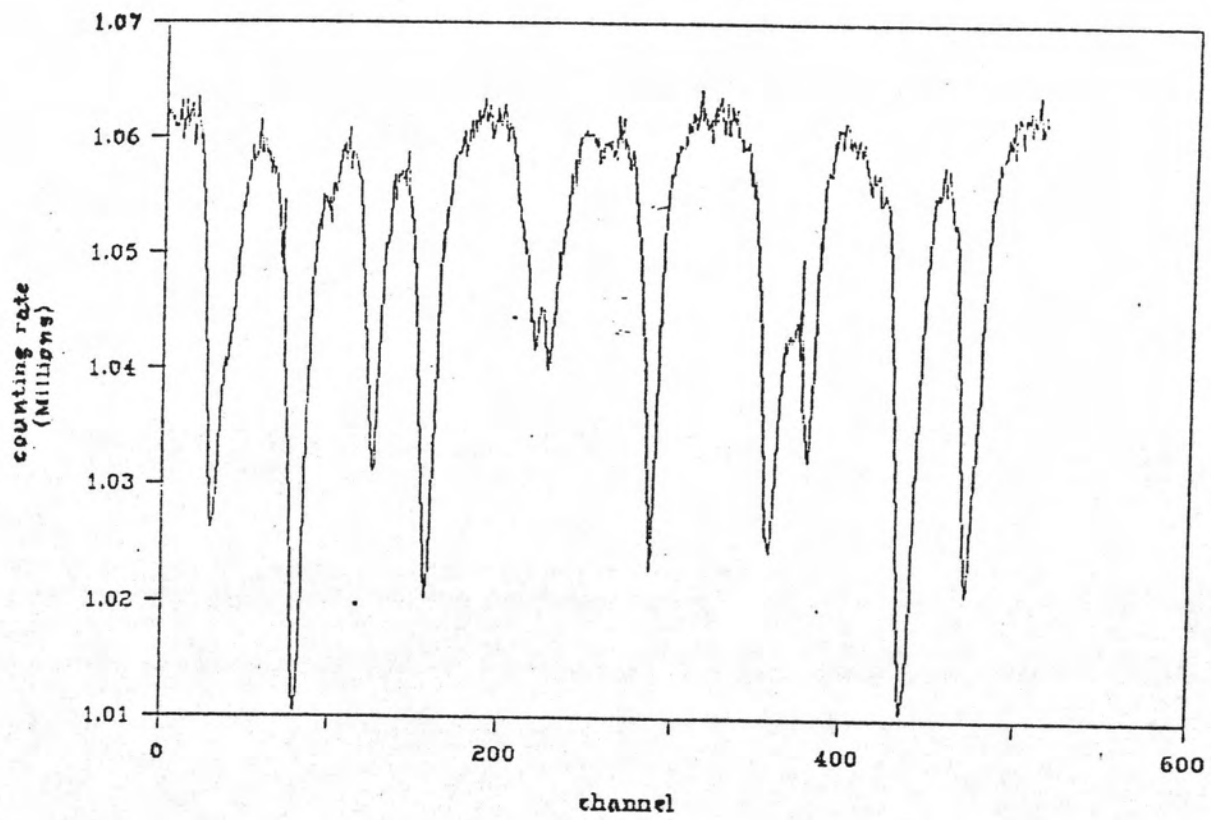


Figure 5.13 The Mössbauer spectra for YIG.